ISSN 1562-6016

УКРАИНА

PROBLEMS OF ATOMIC SCIENCE AND TECHNOLOGY

ВОПРОСЫ АТОМНОЙ НАУКИ И ТЕХНИКИ

ПИТАННЯ АТОМНОЇ НАУКИ І ТЕХНІКИ

№ 4(116)

2018

Публикации журнала ***«Вопросы атомной науки и техники»*** индексируются и реферируются в изданиях Thomson Scientific (США):

- Science Citation Index Expanded;
- Journal Citation Reports/Science Edition,

а также в:

- Реферативном журнале ВИНИТИ (Россия);
- Международной базе ядерной информации (МАГАТЭ)

Publications of the journal ***«Problems of Atomic Science and Technology»*** are indexed and abstracted by Thompson Scientific (USA) in the following:

- Science Citation Index Expanded;
- Journal Citation Reports/Science Edition,

and also in:

- Abstract Journal of VINITI (All-Russian Institute of Scientific and Technical Information);
- International Nuclear Information System (IAEA)

Подписной индекс журнала
«Вопросы атомной науки и техники»
в Каталоге периодических изданий Украины «ПРЕССА» - 95067

Интернет-версия журнала:
http://vant.kipt.kharkov.ua

2018

№4(116)

НАЦИОНАЛЬНАЯ АКАДЕМИЯ НАУК УКРАИНЫ
НАЦИОНАЛЬНЫЙ НАУЧНЫЙ ЦЕНТР
«ХАРЬКОВСКИЙ ФИЗИКО-ТЕХНИЧЕСКИЙ ИНСТИТУТ»

ВОПРОСЫ АТОМНОЙ НАУКИ И ТЕХНИКИ

ПИТАННЯ АТОМНОЇ НАУКИ І ТЕХНІКИ

PROBLEMS OF ATOMIC SCIENCE AND TECHNOLOGY

Научный журнал выходит 6 раз в год
Основан в октябре 1998 г.

Серия «Плазменная электроника и новые методы ускорения».
Выпуск 10

Series «Plasma Electronics and New Methods of Acceleration».
Issue 10

Журнал «Вопросы атомной науки и техники» (Украина) создан на основе издававшегося в ННЦ ХФТИ научно-технического сборника с одноименным названием

VALIDATION OF THE NUMERICAL MODEL OF A SPARK CHANNEL EXPANSION IN A LOW-ENERGY ATMOSPHERIC PRESSURE DISCHARGE

K.V. Korytchenko[1], V.S. Markov[1], I.V. Polyakov[1], E.D. Slepuzhnikov[2], R.G. Meleshchenko[2]
[1]National Science Center "Kharkov Institute of Physics and Technology", Kharkov, Ukraine
E-mail: omsroot@kpi.kharkov.ua;
[2]National University of Civil Defence of Ukraine, Kharkov, Ukraine
E-mail: korytchenko_kv@ukr.net

Gas-dynamic expansion of a low-energy atmospheric pressure spark discharge was numerically simulated. The calculated data were compared with experimental results to validate the numerical model. A satisfactory correlation of spark photo images with a simulated spark channel expansion was observed. It was found out that an experimental total light intensity of spark discharge corresponds with spark radiation power. Time histories of a particle number concentration and energy input were calculated. Radial temperature, pressure, density and conductivity profiles at various times were investigated.

PACS: 52.80.Mg

INTRODUCTION

A spark discharge has a lot of fields of using. For example, it applied for ignition of a combustible mixture including a direct detonation initiation, lighting, electrical switching, nanoparticle generation, etc. A complex experimental investigation of spark discharges requires high resolution techniques to measure a spark channel evolution, generated shock wave expansion, chemical components concentration distributions, light intensity, spatial distribution of temperature, pressure, density in spark channel, efficiency of energy deposition, excitation of discharge components, changing in electrical features (conductivity, voltage falling), etc [1 - 3]. Thus experimental spark researches are extremely complicated.

The numerical model of a spark discharge which is convenient for application was recently developed [4 - 6]. A specific feature of the model is its ability to predict a spark channel expansion in the gas when electric circuit parameters, the discharge gap length, and initial thermodynamic gas state are given.

It is important to determine conditions of the model application. The model was successfully validated previously by a high-energy spark discharge where the total spark energy equals about tens of Joules [7]. Now we validate the model when the total discharge energy is below one Joule.

We used experimental data of a channel expansion of a low-energy atmospheric pressure spark discharge in nitrogen [1]. The experimental data include as a time-resolved imaging as electrical study of the discharge. Thus, the capacitance, resistance and inductance of a serial *RLC*-circuit, the length of the discharge gap and initial thermodynamic state of the discharge gas were used as initial conditions in the numerical model. Then we compared the experimental and simulated results of the channel expansion and the total light intensity to validate the model.

THE NUMERICAL MODEL OF A SPARK CHANNEL EXPANSION

Detailed description of the numerical model is given in [4 - 7]. The model can be applied to simulate a spark evolution after breakdown when the initial current-conducting channel is formed. The model describes a spark stage of a gas-dynamic expansion.

The setup was simplified to a one-dimensional problem in cylindrical symmetry where only radial dependencies were modelled. A system of gas dynamic equations (continuity, momentum and energy) was solved for the multicomponent chemically reactive gas mixture (molecular and atomic nitrogen), written as

$$\frac{\partial \rho}{\partial t}+\frac{1}{r}\frac{\partial (r\rho u)}{\partial r}=0\,; \tag{1}$$

$$\frac{\partial \rho u}{\partial t}+\frac{1}{r}\frac{\partial \left[r\left(p+\rho u^2\right)\right]}{\partial r}=\frac{p}{r}\,; \tag{2}$$

$$\frac{1}{r}\frac{\partial\left[r\left(u\left(\rho\varepsilon+\frac{\rho u^2}{2}+p\right)+k_T\frac{dT}{dt}\right)\right]}{\partial r}+ \\ +\frac{\partial\left[\rho\varepsilon+\frac{\rho u^2}{2}\right]}{\partial t}=\sigma E^2-W_{em}\,; \tag{3}$$

$$\frac{\partial y_i}{\partial t}+\frac{1}{r}\frac{\partial (ruy_i)}{\partial r}=\omega_i\,, \tag{4}$$

where ρ is the gas density; u is the velocity, p is the pressure, ε is the internal energy of gas per the mass unit of gas, k_T is the heat conduction coefficient, E is the electric field strength in the discharge channel column, σ is the plasma conductivity in the channel, W_{em} is the discharge energy radiation loss, r is the radial coordinate, t is the time, T is the gas temperature, y_i is the molar concentration of the i-th component (N_2, N), and ω_i is the rate of change of concentration of the i-th component of the mixture due to chemical reactions.

We applied equations of a local thermodynamic equilibrium (LTE) plasma state to find out plasma parameters in a spark discharge conductive channel. Conditions of LTE-model application were checked. In the conductive channel components e, N, N_+, N_{++} have been considered. In the calculated region outside the conductive channel plasma ionization has been neglected. In this region the components N_2, N have been considered.

We used equations of non-equilibrium chemical reactions to calculate components concentration in this region. The energy deposition in the discharge channel was defined by the parameters of electric circuit. The diffusion process was not taken into account.

To calculate the Joule heat deposited into the discharge channel we are supposed to know the current values of the electric field strength E in the discharge channel column and plasma conductivity distribution σ in the plasma channel. It was assumed that only a longitudinal component of the electric field is present in the discharge channel and the field is uniformly distributed across the channel cross-section.

The conductivity distribution in the gas-discharge channel was considered proceeding from the channel-based problem formulation. The highly ionized region was defined from the condition of tenfold exceed of the frequency of Coulomb collisions in comparison with that of elastic collision of electrons with a neutral plasma component (N atoms) as follows [8]

$$N \cdot \sigma_{tr} \le \frac{n_e \cdot \sigma_{Col}}{10}, \quad (5)$$

where σ_{tr} is the transport cross-section of elastic collisions of electrons with a neutral plasma component, N is the neutral plasma component density; n_e is the electron number density, σ_{Col} is the Coulomb collision cross-section.

It was assumed for the model that plasma in a discharge channel is quasi neutral with the ionization degree not exceeding a double one. An electron attachment process was neglected in the model.

The ionization in the discharge channel was calculated using the Saha equation with regard to the single and double ionization of gas with components of e, N, N_+, N_{++}. The electron density n_e and plasma temperature in rated cells were defined by solving the equation system:

$$\frac{n_e n_{N+}}{N_N} = \frac{g_{N+}}{g_N} A \cdot T^{\frac{3}{2}} \exp\left(-\frac{eI_{N+}}{kT}\right); \quad (6)$$

$$\frac{n_e n_{N++}}{n_{N+}} = \frac{g_{N++}}{g_{N+}} A \cdot T^{\frac{3}{2}} \exp\left(-\frac{eI_{N++}}{kT}\right); \quad (7)$$

$$\varepsilon = \frac{3}{2}(N_N + n_{N+} + n_{N++} + n_e)kT + n_{N+} eI_{N+} + n_{N++} eI_{N++} + (N_N + n_{N+} + n_{N++})I_N / 2; \quad (8)$$

$$n_e = n_{N+} + 2n_{N++}; \quad (9)$$

$$\rho_N = (N_N + n_{N+} + n_{N++}) Z_N m_{a.i.m}, \quad (10)$$

where $A = 6.06 \cdot 10^{-21}$ cm^{-3}eV$^{-3/2}$; g_i are the degeneracy of state for the ion i; I_N is the nitrogen molecule dissociation energy; I_{N+}, I_{N++} is the energy of single and double ionization of nitrogen atom; Z_N is the mass number of nitrogen; $m_{a.i.m.} = 1.66 \cdot 10^{-27}$ kg; ρ_N is the atomic nitrogen density, e is the electron charge, n_e is the electron number density; n_+ is the single ionization atom number density; n_{++} is the double ionization atom number density, N_N is the number density of atomic nitrogen, k is the Boltzman constant.

The degeneracy of state for the ion g_i and ionization energy of I_i components were taken from [9]. The plasma conductivity was calculated using the equation [10]

$$\sigma(Z,T) = \frac{96.994 \cdot K_\sigma(Z) \cdot T^{3/2}}{\ln \Lambda} [\Omega^{-1}\text{cm}^{-1}], \quad (11)$$

where $K_\sigma(Z)$ is the dimensionless coefficient; Z is the average ion charge; $\ln\Lambda$ is the Coulomb logarithm.

In the region of strongly ionized plasma (conductive channel) the gas pressure p was calculated using the expression

$$p = (N + n_e + n_+ + n_{++})kT. \quad (12)$$

Resistance R_{sp} of the discharge channel for the current time point was defined by the integration of current conductivity values σ in rated cells using the expression

$$R_{sp} = l_{sp} / \int_0^{r_{ch}} 2\pi r \sigma dr, \quad (13)$$

where l_{sp} is the discharge gap length (channel); r_{ch} is the conductive channel radius.

The electric field strength E was calculated using the expression

$$E = R_{sp} i / l_{sp}. \quad (14)$$

The electrical process in the series RLC circuit was calculated using the equation

$$L\frac{di}{dt} + \left[R_c + R_{sp}(t)\right] \cdot i + \frac{1}{C}\int_0^t i dt = 0, \quad (15)$$

where C is the capacitor capacitance, R_c is the equivalent ohmic resistance of a discharge circuit; L is the equivalent inductance of a discharge circuit.

The radiation discharge energy losses were calculated using the expression

$$W_{em} = \sigma_{SB} T^4 / l_R, \quad (16)$$

where σ_{SB} is the Stefan–Boltzmann constant, l_R is the Rosseland mean free path.

The dissociation/association process in nitrogen gas was calculated by reaction (Table). The velocity constant of the chemical reaction is expressed as

$$k_k = A_k T^{n_k} \exp\left(\frac{-E_{ak}}{RT}\right), \quad (17)$$

where R is the gas constant.

The coefficients of the velocity constants of forward reactions and the activation energy, adopted for the model

REACTION	A_k	n_k	E_{ak}
$N_2 + M \leftrightarrow N + N + M$	$8.508 \cdot 10^{25}$	-2.5	225
Remark. Where M denotes the third particle. The values are expressed in calories, moles, cm^3, and s			

The reverse rate coefficient was calculated from the forward rate and the equilibrium constant.

Specific heat capacity at constant pressure, standard-state molar enthalpy and standard-state molar entropy component (N_2, N) as a function of a temperature T in the range of 300 to 5000 K were calculated as in [12]. The energy of the unit of mixture volume U_0 was prescribed by the expression of

$$\rho\varepsilon = \sum_k y_k U_k^0, \quad (18)$$

where y_k is the molecular concentration of the k-th component of mixture, U_k^0 is the internal energy of 1 mole of the k-th component.

A mixture pressure in the cells outside the conductive channel was calculated using the sum of partial

pressures of mixture components. The gradients of thermodynamic gas parameters are assumed to be absent for the discharge channel axis in a cylindrical symmetry. The computational area size was prescribed in the manner of preventing disturbance from reaching the right boundary. It is assumed that initial conditions have no gas dynamic perturbations in the entire computation region. For the computations given below it is assumed that $p_0 = 1.013 \cdot 10^5$ Pa, $T_0 = 300$ K. For initial conditions the computation region was filled with molecular nitrogen. The model requires a circuit shorting to start simulating. So we manually inputted an energy in the simulated region with a radius of $r_0 = 50$ μm during a time of t = 10 ns to form a narrow current-conducting channel. This energy was 0.24 mJ.

RESULTS OF A NUMERICAL SIMULATION OF A SPARK EXPANSION

It is accustomed getting the schlieren images to investigate a spark channel expansion [3]. The Schlieren images show a spatial distribution of density gradient that allows being visible as a channel as a shock wave due to density changing in the channel and the wave during a spark evolution. The photo images taken from work [1] show a spatial distribution of lighting intensity in spark discharge. It is known [8] that a high-temperature spark channel produces the lighting. Thus we compared the photo images with the radial temperature profiles of a spark discharge in this work. We used the photo imaging results for flat-end electrodes because this data better corresponds to a one-dimensional simulation in cylindrical symmetry assumed in our model. The length of the spark gap l equaled 2 mm in the calculation that corresponds to the experimental condition of the shooting.

The parameters of a serial *RLC* circuit used in [1] were analyzed carefully. We applied a capacitor bank with a total capacitance of $C = 29$ nF and inductance of $L = 3.6$ μH in the calculation. The charge voltage was $U_c = 5425$ V thus the total energy was 427 mJ. According to estimation presented in [1], the total resistance values were in the range of 1.30...1.65 Ω. Using the measured current signal and simulating a current curve for such a *RLC* circuit where the resistance was R = 1.65 Ω we found out that there is a correlation of the current curves in third period of discharge (Fig. 1).

Initially we assumed that the resistance value of 1.65 Ω is the equivalent ohmic resistance of discharge circuit. And the current reducing happened due to an additional resistance of a spark discharge.

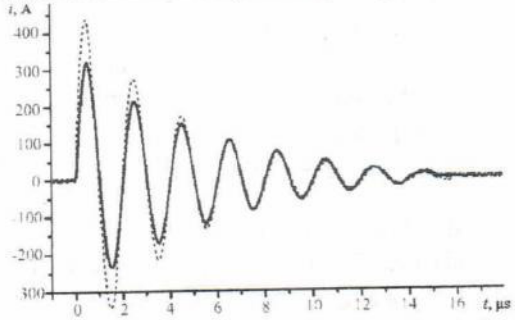

Fig. 1. Experimental current signal [1] (solid curve) and calculated current (dotted curve) for $R_c = 1.65$ Ω

But our simulated data obtained by taking into account the spark resistance showed that the calculated amplitude of a discharge current exceeded the experimental amplitude in this case. Current difference was above 100 A. Moreover, we observed that the simulated current-conducting channel expanded faster than the measured spark channel. For example, a comparison between the image at 2750 ns and radial temperature profile at 2000 ns is given (Fig. 2).

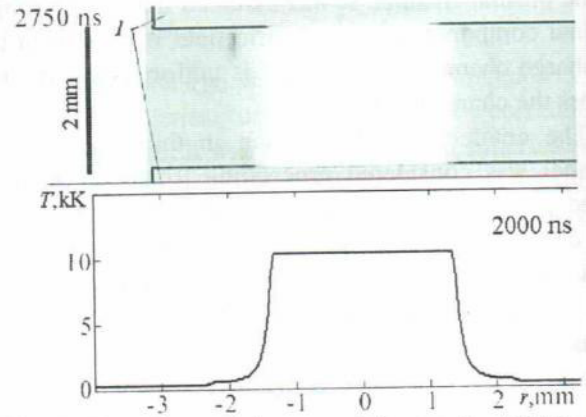

Fig. 2. Experimental images of the spark at 2750 ns and calculated radial temperature profile at 2000 ns

So the ohmic resistance was adapted in such a way that we had a satisfactory correlation of the measured discharge current with the simulated current. The ohmic resistance was variable. The resistance was presented by function of time (Fig. 3).

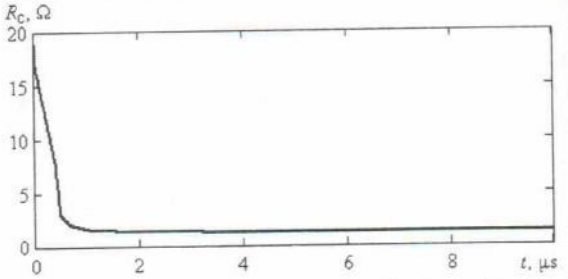

Fig. 3. Time dependence of the ohmic resistance adapted for the calculation

It is known [3] that there is a voltage drop in anode and cathode zones that is variable during a spark evolution. Thus the time variable ohmic resistance can be caused by a process connected with discharge electrodes.

A comparison of the experimental and calculated discharge currents is presented (Fig. 4).

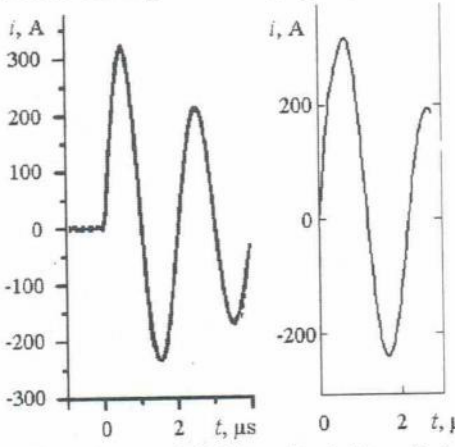

Fig. 4. Experimental [1] (on the left) and simulated (on the right) spark current

The numerical simulation showed that the photo images of spark discharge present the evolution of high-temperature region of the discharge where gas temperature exceeds 10000 K (Figs. 5-7).

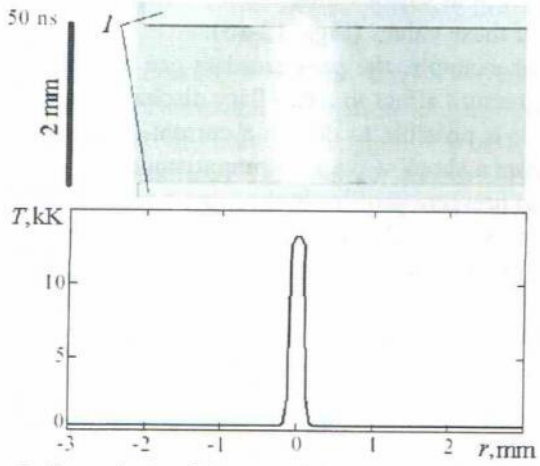

Fig. 5. Experimental image of the spark (upper) and calculated radial temperature profile (below) at 50 ns

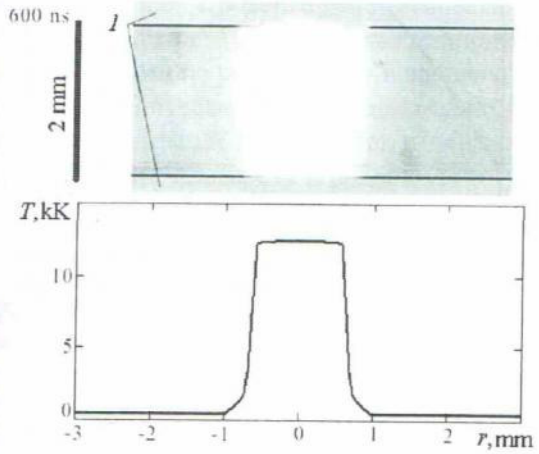

Fig. 6. Experimental image of the spark (upper) and calculated radial temperature profile (below) at 600 ns

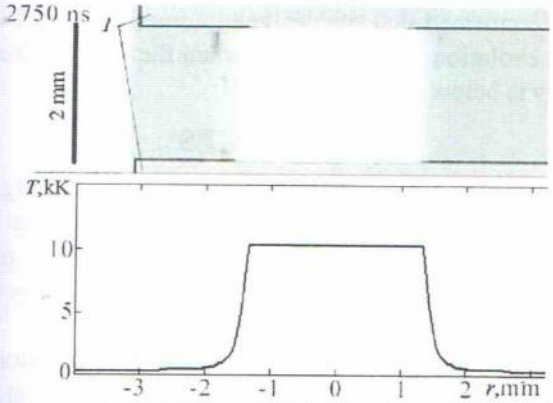

Fig. 7. Experimental image [1] of the spark (upper) and calculated radial temperature profile (below) at 2750 ns

There is temperature growth behind shock wave that is not visible in the images. The temperature rises in the range of 460...500 K behind the shock wave at 2750 ns (see Fig. 5). It is known [8] that when gas temperature is slightly higher than room temperature, gas has a specific absorption/emission spectrum. Thus the temperature growth caused by the wave is not visible because the preheated gas does not have visible spectrum.

The comparisons show that we have a satisfactory agreement between experiment and theory.

Radiant energy of the investigated discharge was calculated (Fig. 8).

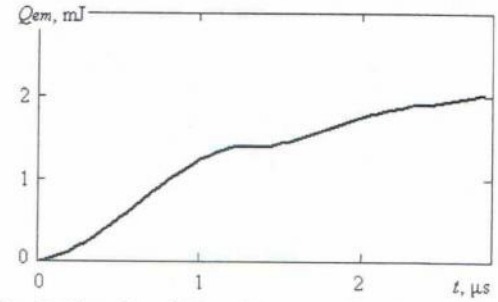

Fig. 8. Simulated time history of radiant energy

Then we differentiated the radiant energy with respect to time to calculate radiant power. As a result we clarified that normalized intensity obtained in work [1] corresponds to the spark radiant power. A maximum of the power exceeds 1.5 kW (Fig. 9).

Practically the same evolution of spark channel radiuses we have in experimental and calculated cases (Fig. 10). There is a slight difference at initial time of the channel expansion. It is known [8] that there is a spark process of current contraction happens after breakdown. We think a time resolution of an experimental setup did not allow catching a contraction process.

The numerical model allows investigating a time history of a particle number concentration (Fig. 11). These results can be useful to check the model using specific experimental equipment.

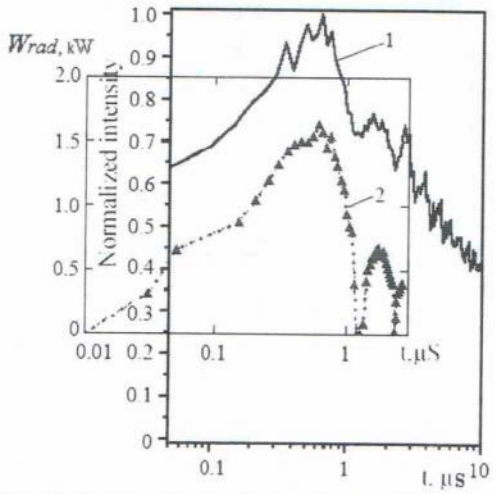

Fig. 9. Comparison of experimental intensity of lighting [1] (curve № 1) and calculated radiation power (curve № 2)

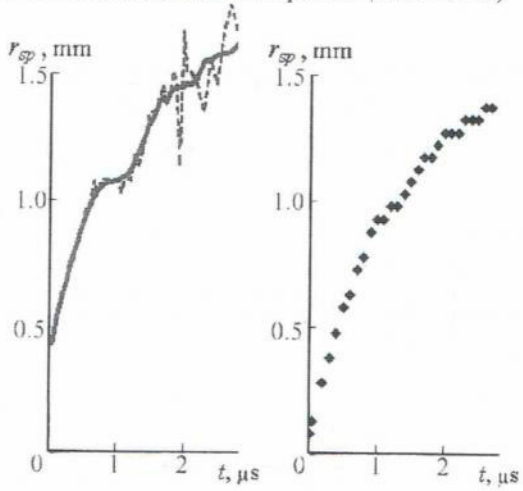

Fig. 10. Comparison of evolutions of spark channel radius in experimental [1] (on the left) and calculated (on the right) cases

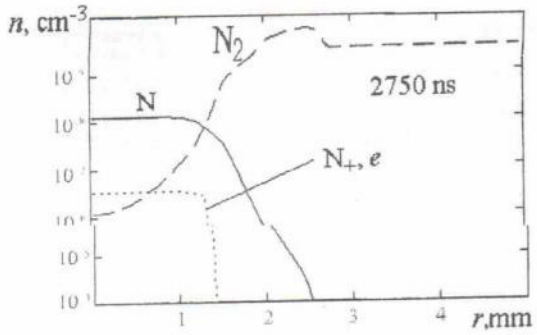

Fig. 11. The simulated radial profiles of a particle number concentration in the spark discharge at 2750 ns

A time variation of a spark resistance was calculated (Fig 12). It was found out that the spark resistance in 0.2…0.3 μs falls below 1 Ω.

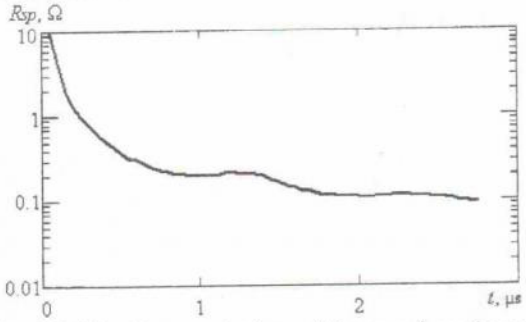

Fig. 12. The time variation of the spark resistance

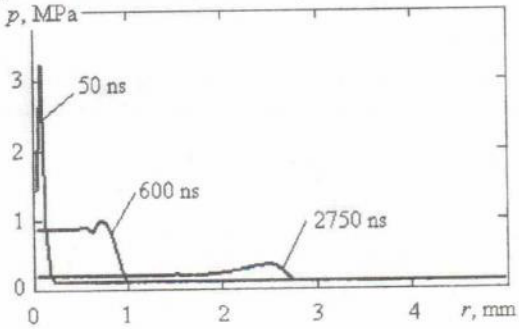

Fig. 13. The simulated radial pressure profiles atvarious times

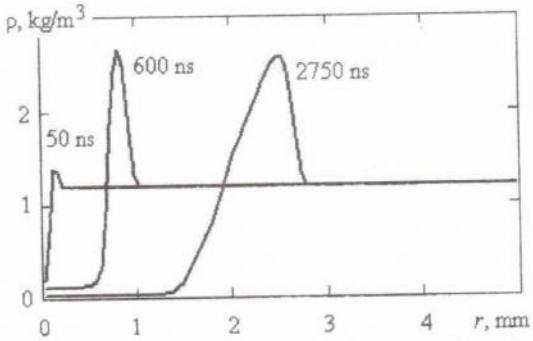

Fig. 14. The radial density profiles at various times

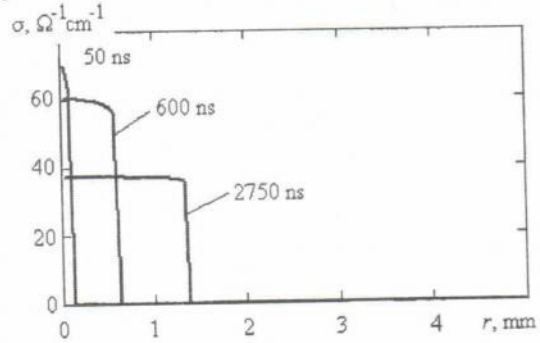

Fig. 15. The radial conductivity profiles at various times

It is a reason that the spark resistance weakly influences the discharge current in the considered case. There is a technical problem to get experimental measurements of pressure, density and conductivity in spark discharges at various times. We presented the simulated data of these values (Figs. 13-15).

For example, the pressure data can be useful to predict pressure affect in a capillary discharge. As for other data, it is possible to detach a current-conducting channel from a shock wave via comparison of the conductivity and pressure profiles at the same time.

It is known [8] that spark energy efficiency is variable. The efficiency depends on total discharge energy, electrical circuit parameters, a length of a spark gap, and an initial thermodynamic gas state in discharge, etc. The designed model allows finding out energy inputted in a spark channel (Fig. 16).

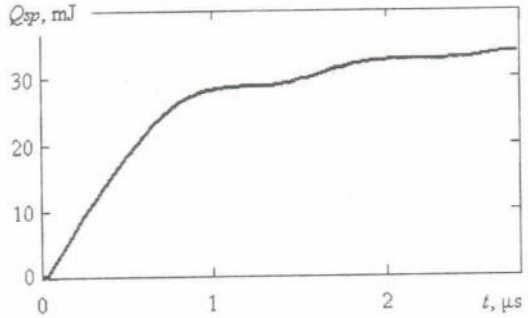

Fig. 16. The simulated time history of energy input in spark discharge

We calculated that an intensive energy input happens at first period of discharge. The efficiency exceeds 8% in considered case.

CONCLUSIONS

A satisfactory correlation between spark photo images and simulated radial temperature profiles at various times confirmed that the designed numerical model of a spark evolution can be applied when the total discharge energy is below one Joule.

REFERENCES

1. J. M. Palomares, A. Kohut, G. Galbács, R. Engeln, and Zs. Geretovszky. A time-resolved imaging and electrical study on a high current atmospheric pressure spark discharge // *Journal of Applied Physics*. 2015, v. 118, p. 233305.
2. S. Essmann, D. Markus, U. Maas. Investigation of the spark channel of electrical discharges near the minimum ignition energy // *Plasma Physics and Technology*. 2016, №3, p. 116-121.
3. N.M. Gegechkori. Experimental studies of spark discharge channel // *Journal of Experimental and Theoretical Physics*. 1951, №4, v. 21, p. 493-506.
4. K.V. Korytchenko. High-voltage electric discharge technique for the generation of shock waves and heating the reacting gas. *Dr. Sc. Thesis National Technical University "Kharkov Polytechnic Institute"*, 2014.
5. K.V. Korytchenko, E.V. Poklonskii, P.N. Krivosheev. Model of the spark discharge initiation of detonation in a mixture of hydrogen with oxygen // *Russ. J. Phys. Chem. B*. 2014, № 8, p. 692-700.

6. K.V. Korytchenko, V.I. Golota, D.V. Kudin, O.V. Sakun. Numerical simulation of the energy distribution into the spark at the direct detonation initiation // *Problems of Atomic Science and Technology. Series "Nuclear Physics Investigations"*. 2015, №3, p. 154-158.
7. K.V. Korytchenko, E.V. Poklonskiy, D.V. Vinnikov, D.V. Kudin. Numerical simulation of gas-dynamic stage of spark discharge in oxygen // *Problems of Atomic Science and Technology. Series "Plasma Electronics and New Methods of Acceleration"*. 2013, № 4, p. 155-160.
8. Yu.P. Raiser. *Gas discharge physics*. M.: "Nauka", 1987, 592 p.
9. Myron N. Plooster. Shock waves from line sources // *report NCAR-TN-37*, November, 1968.
10. S.I. Braginski. On the theory of spark channel development // *Journal of Experimental and Theoretical Physics*. 1958, v. 34, № 6, p. 1548-1557.
11. S.I. Drabkina. On the theory of development of spark discharge channel // *Journal of Experimental and Theoretical Physics*. 1951, v. 21, № 4, p. 473-483.
12. E.L. Petersen, R.K. Hanson. Reduced Kinetics Mechanisms for Ram Accelerator Combustion // *Journal Prop. and Power*. 1999, v. 15, № 4, p. 591-600.

Article received 01.06.2018

ПРОВЕРКА МАТЕМАТИЧЕСКОЙ МОДЕЛИ РАСШИРЕНИЯ ИСКРОВОГО КАНАЛА НИЗКОЭНЕРГЕТИЧНОГО РАЗРЯДА АТМОСФЕРНОГО ДАВЛЕНИЯ

К.В. Корытченко, В.С. Марков, И.В. Поляков, Е.Д. Слепужников, Р.Г. Мелещенко

Численно исследовано газодинамическое расширение низкоэнергетического искрового разряда атмосферного давления. Проверка математической модели проведена путем сравнения численных и экспериментальных результатов. Получена удовлетворительная корреляция фотоизображений искрового разряда с расчетными данными по расширению искрового канала. Выявлено, что полная интенсивность излучения искрового разряда, получаемая экспериментально, соответствует мощности излучения искры. Рассчитано распределение концентрации компонентов и динамика ввода энергии в искру. Исследованы распределения температуры, давления, плотности и проводимости в радиальном сечении в разные моменты времени.

ПЕРЕВІРКА МАТЕМАТИЧНОЇ МОДЕЛІ РОЗШИРЕННЯ ІСКРОВОГО КАНАЛУ НИЗЬКОЕНЕРГЕТИЧНОГО РОЗРЯДУ АТМОСФЕРНОГО ТИСКУ

К.В. Коритченко, В.С. Марков, І.В. Поляков, Є.Д. Слепужніков, Р.Г. Мелещенко

Чисельно досліджено газодинамічне розширення низькоенергетичного іскрового розряду атмосферного тиску. Перевірка математичної моделі проведена шляхом порівняння чисельних та експериментальних результатів. Отримана задовільна кореляція фотозображень іскрового розряду з розрахунковими даними з розширення іскрового каналу. З'ясовано, що повна інтенсивність випромінювання іскрового розряду, яка отримана експериментально, відповідає потужності випромінювання іскри. Розраховано розподіл концентрації компонентів та динаміка вводу енергії в іскру. Досліджені розподіли температури, тиску, густини та провідності в радіальному розрізі в різні моменти часу.

CONTENTS

NONRELATIVISTIC ELECTRONICS

RELATIVISTIC ELECTRONICS

ADVANCED METHODS OF ACCELERATION

THERMONUCLEAR FUSION (COLLECTIVE PROCESSES)

COLLECTIVE PROCESSES IN SPACE PLASMAS

PLASMA-BEAM DISCHARGE, DISCHARGE AND PLASMACHEMISTRY